REFINEMENT OF 3D DOPPLER VELOCITY USING 3D WINDPROFILER DATA

Yong Zhang, John L. Barron, Robert E. Mercer
{**yzhan433,barron,mercer**}**@csd.uwo.ca**
Dept. of Computer Science, University of Western Ontario
London, Ontario, Canada, N6A 5B7

Abstract: We present a preliminary report on combining the data from a Windprofiler radar and a NEXRADII Doppler radar to compute 3D optical flow. Previously, we computed 3D optical flow from 3D Doppler radar radial velocity data only. Windprofiler data improves the recovery of the velocity component in the upwards direction, where Windprofiler data is believed to be more accurate.

Keywords: Doppler Radial Velocity, 3D Optical Flow, Doppler Radial Velocity, Windprofiler Velocity, Least Square Optical Flow, Regularized Optical Flow

1 Introduction

Doppler radar is an important meteorological observation tool. In order to gain knowledge of how storms move over time, much research have been devoted to retrieving 3D full velocity from the observed radial velocity (for example, Lhermitte and Atlas [LA61], Easterbrook [Eas75] and Waldteufel and Corbin [WC79]). Rather than using the traditional methods provided by meteorologists, our research group is solving this problem using the 3D Optical Flow framework [BRCJ05], which is a technology widely applied in the Computer Vision area. In this paper, we "refine" 3D Doppler optical flow by integrating Windprofiler data into the calculation. We illustrate this refinement using data from the Detroit NCDC Doppler and the Harrow Windprofiler radars.

We use a right-handed coordinate system where the x and y axes describe a plane and the z axis the height of the data. Optical flow is a 3D vector field, (U, V, W), and is the 3D motion of water precipitation over time. At lower elevation angles in the data, we note that the W velocity component is almost orthogonal to the radial velocities: in the presence of even small amounts of noise, radial velocity contains little W information and is difficult to recover.

2 The Optical Flow Calculation

We have devised a 3D regularization solution based on an extension of Horn and Schunck's 2D optical flow regularization algorithm [HS81]. That is, a number of constraint terms on 3D velocity are minimized (regularized) over the 3D domain.

The 1^{st} term we use is the 3D **Radial Velocity Constraint**, which requires that the full velocity projected in the radial direction be the radial velocity:

$$\vec{V} \cdot \hat{r} = V_r, \tag{1}$$

where $\vec{V} = (U, V, W)$ is the local 3D velocity (which we want to compute), $\hat{r}$ is the local unit radial velocity direction (which we know precisely from the structure of the radar data) and V_r is the measured local radial velocity magnitude.

The 2^{nd} constraint is a 3D Horn and Schunck like **Velocity Smoothness Constraint**, which requires that velocity vary smoothly everywhere by keeping velocity component derivatives in the 3 dimensions as small as possible.

A 3^{rd} constraint is based on an extension of the 2D Lucas and Kanade least squares optical flow algorithm [LK81] into 3D. This algorithm assumes that 3D velocity is locally constant in local neighbourhoods but that the local radial velocity varies in these $N \times N \times N$ neighbourhoods. A least squares calculation is then performed for each neighbourhood:

$$\underbrace{\begin{bmatrix} r_{X1} & r_{Y1} & r_{Z1} \\ r_{X2} & r_{Y2} & r_{Z2} \\ \cdots & \cdots & \cdots \\ \cdots & \cdots & \cdots \\ r_{XN} & r_{YN} & r_{ZN} \end{bmatrix}}_{A} \begin{bmatrix} U_{ls} \\ V_{ls} \\ W_{ls} \end{bmatrix} = \begin{bmatrix} V_{r1} \\ V_{r2} \\ \cdots \\ \cdots \\ V_{rN} \end{bmatrix}. \qquad (2)$$

If matrix $A^T A$ can be reliably inverted the least squares velocity $\vec{V}_{ls} = (U_{ls}, V_{ls}, W_{ls})$ can be recovered. This allows us to use a **Least Squares Velocity Consistency Constraint**, which requires computed velocities to be consistent with local least squares velocities.

A 4^{th} **Windprofiler Velocity Consistency Constraint** incorporates the Windprofiler velocity estimates, $\vec{V}_{wp}$, into the regularization, again by requiring local values of $\vec{V}_{wp}$ and $\vec{V}$ be consistent.

The complete regularization functional is the sum of these constraints:

$$\int\int\int \Bigg(\underbrace{(\vec{V} \cdot \hat{r} - V_r)^2}_{Radial\ Velocity\ \ Constraint} + \\ \alpha^2 \underbrace{(U_X^2 + U_Y^2 + U_Z^2 + V_X^2 + V_Y^2 + V_Z^2 + W_X^2 + W_Y^2 + W_Z^2)}_{Velocity\ Smoothness\ Constraint} + \\ \beta^2 \underbrace{((U - U_{ls})^2 + (V - V_{ls})^2 + (W - W_{ls})^2)}_{Least\ Squares\ Velocity\ Consistency\ Constraint} + \\ \sum_{i=1}^{n} \gamma_i^2 \underbrace{((U - U_{wp_i})^2 + (V - V_{wp_i})^2 + (W - W_{wp_i})^2)}_{Windprofiler\ Velocity\ Consistency\ Constraint} \Bigg) \partial X \partial Y \partial Z, \qquad (3)$$

where γ is the Lagrange multiplier for this additional constraint. The value of γ_i at each voxel is calculated from a 3D Gaussian function based on the distance between it and the location of the i^{th} point of the Windprofiler radar:

$$\gamma_i = \frac{\Gamma}{(2\pi)^{\frac{3}{2}} \prod_{k=1}^{3} \sigma_k} e^{-\left(\frac{(x - x_{wp_i})^2}{2\sigma_1^2} + \frac{(y - y_{wp_i})^2}{2\sigma_2^2} + \frac{(z - z_{wp_i})^2}{2\sigma_3^2}\right)}. \qquad (4)$$

$\sigma_1, \sigma_2, \sigma_3$ are the three standard deviations that specify the shape of the 3D Gaussian distribution according to the distance between the points where $\vec{V}$ and $\vec{V}_{wpi}$ are measured in each of the 3 dimensions, while $\Gamma = 1000$ is a preset constant value. For our experiments, σ_1 and σ_2 have the value 20.0, reflecting the large x and y range of values, while $\sigma_3 = 0.4$, reflecting the much smaller range in the z values. The "goodness" of these parameter values are confirmed by synthetic and real data experiments.

We use Gauss-Seidel iterations on the Euler-Lagrange equations derived from Equation (3) to compute the flow. At the start of the iterations, $\vec{V}^0$ is set to zero. Until a fixed number of iterations (150) or while the difference between the k^{th} and $(k+1)^{th}$ velocity fields remains greater than a threshold $\tau = 10^{-3}$, the iterative calculation continues. At the end, the velocity field is set to the last iteration's velocity field. We refer to this as the **refined** optical flow while the original optical flow without the Windprofiler constraint is referred to the **unrefined** optical flow [BRCJ05].

3 Experimental Results

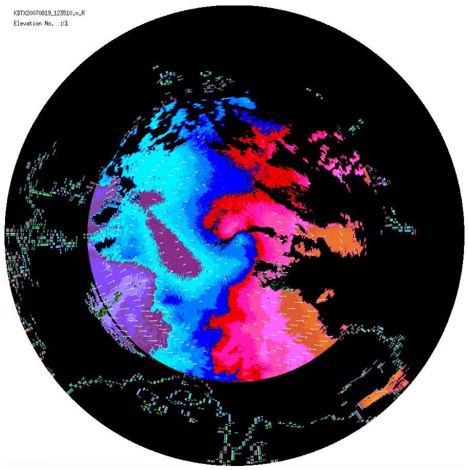

(a)

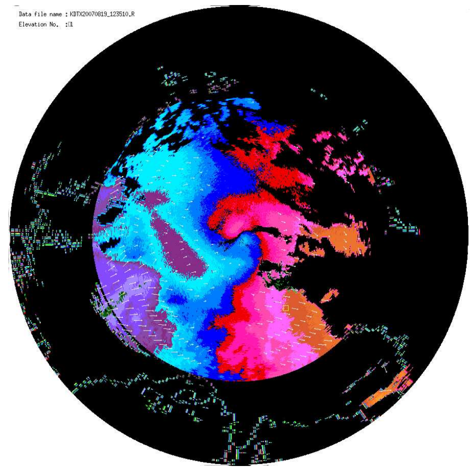

(b)

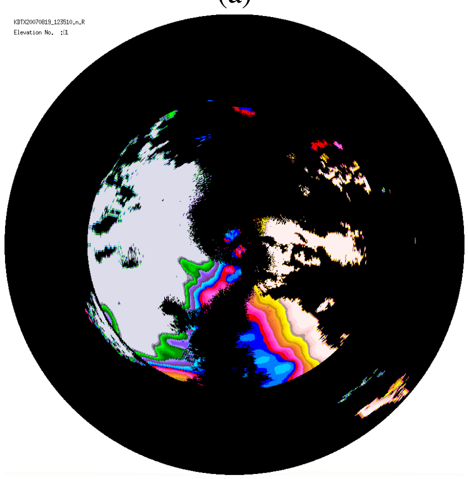

(c)

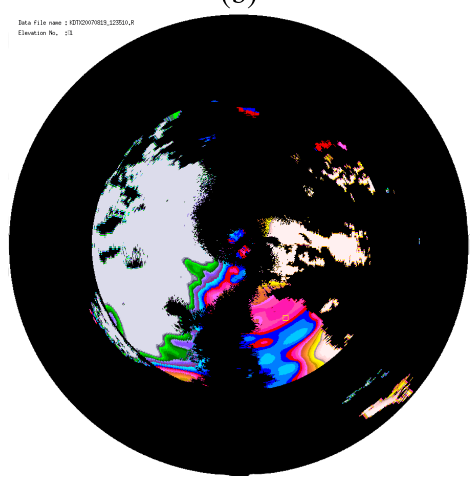

(d)

Figure 1: Full velocity retrieved from the Detroit Doppler (and the Harrow Windprofiler) data on August 19^{th}, 2007 at 12:35:10: (a) the unrefined UV optical flow, (b) the refined UV optical flow, (c) the W component of the unrefined optical flow and (d) the W component of the refined optical flow.

We present some preliminary results for our measured Doppler and Windprofiler data. Figures 1a and 1b show the unrefined and refined UV optical flow fields for the Detroit Doppler data at $12:35:10$ of August 19^{th}, 2007. The yellow square in the bottom-right quadrant (near the origin) in these Figures indicates the position of the Harrow Windprofiler radar relative to the Detroit Doppler radar. We also show the W component of optical flow along the z (height) axis in Figures 1c and 1d. Component velocities in these figures are shown as coloured pixels, whose correspondence with numerical values is the standard used for NEXRADII data. Note that these component colours have replaced the radial velocity magnitude colours in Figures 1a and 1b.

It is clear from the z component flow field images that the refined method significantly changes the flow field around the Windprofiler radar. Figure 1a has the unrefined flow going north while Figure 1c has the refined flow going south. We see a significant change in the recovery of component velocity W in the z direction. In the unrefined component flow shown in Figure 1c, there is a large area where the component velocities have reached their maximum value (yellow). However, in the component flow shown in Figure 1h, it is obvious that a more reasonable result has been obtained in the area surrounding the Windprofiler radar. We observe a major upward velocity component in the areas not overlapped by the Windprofiler radar but a significant downward velocity component in outer area around the Windprofiler radar. This is due to the fact that the Windprofiler constraint adopted different velocity values for the Doppler voxels according to their actual distances from the Doppler radar points.

4 Conclusions and Future Work

In this paper we briefly described how Windprofiler data at the Harrow radar station could be combined with NEXRADII Doppler data from Detroit to produce arguably more accurate optical flow field in the vicinity of the Windprofiler radar. We showed that qualitatively, more accurate and detailed information could be recovered along the z (depth) dimension and sometimes in the x and y dimensions. However, it is noted that a Windprofiler radar only covers a small overlapping area compared to a Doppler radar. This limits its application. Our framework can handle more Windprofiler radars but we do not yet have data for more than one overlapping Windprofiler and Doppler radars. Using multiple Doppler and Windprofiler radars over time is one current area of research. We are also currently constructing "realistic" Doppler and Windprofiler synthetic data and performing a quantitative analysis to determine the actual accuracy improvements of refined flow over unrefined flow.

References

[BRCJ05] J.L. Barron, R.E.Mercer, X. Chen, and P. Joe. 3d velocity from 3d doppler radial velocity. *Intl. Journal of Imaging Systems and Technology*, 15:189–198, 2005.

[Eas75] C. C. Easterbrook. Estimating horizontal wind fields by two-dimensional curve fitting of single doppler radar measurements. In *16th Radar Meteorology Conference*, pages 214–219, 1975.

[HS81] B.K.P. Horn and B.G. Schunck. Determing optical flow. *Artifical Intelligence*, 17:185–204, 1981.

[LA61] R. M. Lhermitte and D. Altas. Precipitation motion by pulse doppler. In *Ninth Weather Radar Conference*, pages 218–223, 1961.

[LK81] B.D. Lucas and T. Kanade. An iterative image-registration technique with an application to stereo vision. In *DARPA Image Understanding Workshop*, pages 121–130, 1981.

[WC79] P. Waldteufel and H. Corbin. On the analysis of single-doppler radar data. *Journal of Applied Meteorology*, 18:532–542, 1979.